

# Partial Volume Correction using an Energy Multiresolution Analysis

Francisca P. Figueiras, Xavier Jimenez, Deborah Pareto, Juan D. Gispert

**Abstract**—Position Emission Tomography (PET) allows the in-vivo monitoring of functional processes in the body. However its limited spatial resolution induces Partial Volume Effect (PVE), which leads to a loss of signal in tissues of size similar to the Point Spread Function (PSF) of the imaging device and induces activity spillover between adjacent structures with different amounts of activity. The aim of Mutual Multiresolution Approach (MMA) is to introduce the high frequency information of an anatomical image into the functional image in order to achieve a higher resolution PET and to decrease PVE. Nevertheless, the anatomical details (high frequency MRI wavelet coefficients) can not be directly replaced into the functional image since they do not have the same spatial resolution neither the same wavelet coefficient intensities. Thus the process relies on a wavelet-based image merging, and aims at detecting, modifying and incorporating high resolution details of the MRI into the PET. In this work a Partial Volume Correction (PVC) algorithm was implemented based on the decomposition of two co-registered PET and MR images using a three-dimensional Discrete Wavelet Transform (3D DWT) and on both wavelet coefficient energies. To validate the performance of the proposed PVC design, regarding the quantitative measurements, the NEMA Image Quality phantom was used. Finally, in order to demonstrate the use of the algorithm in clinical context, the technique was also applied to a  $^{18}\text{F}$ -FDG study of a patient with severe leukariosis, having already a T-1 weighted 3D MRI scan. The quantitative results demonstrate that the combination of MMA and the energy image analysis leads to a significant recovery of lost intensity induced by PVE. Results from this work are encouraging, however it presents its own limitations since it introduces an artifact in the final corrected functional image.

## I. INTRODUCTION

POSITRON Emission Tomography (PET) allows the in-vivo monitoring of functional processes in the body. However its limited spatial resolution induces Partial Volume Effect (PVE), which leads to a loss of signal in tissues of size similar to the Point Spread Function (PSF) of the imaging device and induces activity spillover between adjacent structures with different amounts of activity [1-4].

Manuscript received May 11, 2009.

This work was partially supported by the Ministerio de Industria, Turismo y Comercio (Cenit-Ingenio Program: CDTEAM project). F. P. Figueiras has a PhD fellowship from the Fundação para a Ciência e a Tecnologia (Ministério da Ciência, Tecnologia e Ensino Superior – Portugal).

F. P. Figueiras, X. Jimenez, D. Pareto and J. D. Gispert are with the Institut d'Alta Tecnologia - Parc de Recerca Biomèdica de Barcelona (PRBB), CRC Corporació Sanitària. Dr. Aiguader 88 08003 Barcelona, Spain. (corresponding author telephone: +34 935511600, e-mail: jgispert@crcorp.es).

D. Pareto and J. D. Gispert are also with the CIBER en Bioingeniería, Biomateriales y Nanomedicina (CIBER-BBN). C/ María de Luna 11 Edificio CEEI 50018 Zaragoza, Spain.

There exists a wide variety of algorithms aiming at correcting PVE. PVE can be corrected using either region of interest or voxel based approaches. Most of the Partial Volume Correction (PVC) methods imply the use of *a priori* information provided either by MRI or CT. One of the reference methods, described by Rousset *et al* [1], allows an estimation of the real mean signal in any homogeneous tissue providing that its true boundaries are known. This can be achieved by mostly a manual contouring of the tissue of interest on the CT or MR image, but the homogeneous assumption of the region of interest remains questionable and relies only on visual analysis of the PET image. Moreover, an adequate tissue correlation between PET and MRI or CT is mandatory and difficult to achieve in certain circumstances because of patient physiological motion as well as patient uncontrollable movement in a more general sense between and during image acquisitions. Additional problems on the use of anatomical information for PVE correction include differences in the appearance and size of some tumors (or structures in general) between the functional and the anatomical images, since they provide different information.

Boussion *et al* [3] proposed a new voxel wise based PVE correction methodology based on mutual multiresolution analysis (MMA) of an emission tomography image and a corresponding co-registered CT or MRI image. The aim of MMA is to introduce the high frequency information of an anatomical image into the functional image in order to achieve a higher resolution PET and to decrease PVE. The technique proposed by Boussion *et al* [3] is able to carry out adequate correction without drawing regions of interest. In addition, the creation of PVE corrected images allows the performance of further image processing. On the other hand, this methodology involves mutual wavelet analysis of PET and a co-registered anatomical image, consequently suffering from the limitations related to the tissue spatial correlation described above.

Recently, Shidahara *et al* [4] implemented a new method to replace the high resolution components of the PET image by those of the anatomical image. They used a local scaling including three different parameters:  $\beta$  is applied to all the wavelet coefficients in order to compensate the difference between MRI and PET spatial resolution; Due to the different intensity of wavelet coefficients between PET and the anatomical images, a scaling parameter  $\alpha$  is calculated and applied only to the higher frequency details of the MRI; Finally, a branching ratio  $\gamma$  is introduced to weight the anatomical information versus the noise.

In this work a PVC algorithm was implemented based on the decomposition of two co-registered PET and MR images using a three-dimensional Discrete Wavelet Transform (3D DWT) and on both wavelet coefficient energies.

## II. MATERIALS AND METHODS

As a first stage, it is presented the principal of the MMA algorithm, which is extensively described in [3]. The process relies on a wavelet-based image merging, and aims at detecting, modifying and incorporating high resolution details of the MRI into the PET (MRI is taken as an example, but the methodology is exactly the same when considering CT as the anatomical image).

### A. Wavelet Transform and PVC Algorithm

Although the theoretical foundations of multiresolution analysis do not constitute the main topic of this study, it is constructive to introduce the basic concepts of the wavelet transform which is an important part of the proposed methodology. Actually, the wavelet transform can be introduced by comparison with the more common Fourier transform with which it has a number of similarities. While the Fourier transform provides global information about the spatial frequencies in an image, the wavelet transform leads to a local representation of these spectral properties. From an image processing point of view, the Fourier transform permits one to switch between the spatial and the frequency domains while the wavelet transform allows one to bring them together in one single image. In practice, the wavelet transform of a given image is another image presenting the areas where one may find either more or less important contrast. In addition, one of the interests of the wavelet transform in image processing is that it enables work at different levels of spatial resolution, operating as a tool of multiresolution analysis. Multiresolution analysis allows retrieving the layers of details that have different sizes by separating the spatial frequencies that the image contains. Basically, a medical image at a given spatial resolution  $R$  contains information at different scales, from large structures to small details. For instance, in a cerebral MRI the sharp edges between white and grey matters will be lost when a low-pass filter is applied, but at the same time the skull will stay clearly separated from the brain [3].

In this work the discrete wavelet transform (DWT) was used. The analysis filter bank (one-dimensional DWT) decomposes a input signal into two subband signals,  $h_0$  and  $h_1$ . The signal  $h_0$  represents the low frequency (or coarse) part of the input signal, while the signal  $h_1$  represents the high frequency (or detail) information. The analysis filter bank first filters the input signal using a lowpass and a highpass filter and then the output of each filter is down-sampled by 2 to obtain the two subband signals,  $h_0$  and  $h_1$ .

For medical imaging processing it is necessary to use the a three-dimensional DWT (3D DWT). In the 3D case, the one-dimensional analysis filter bank is applied in turn to each of the three dimensions. If the data is of size  $N_1$  by  $N_2$  by  $N_3$ , then after applying the 1D analysis filter bank to the first dimension we have two subband data sets, each of size  $N_1/2$  by  $N_2$  by  $N_3$ . After applying the 1D analysis filter bank to the second dimension we have four subband data sets, each of size  $N_1/2$  by  $N_2/2$  by  $N_3$ . Applying the 1D analysis filter bank to the third dimension gives eight subband data sets (one low subband and seven high frequency subbands), each of size  $N_1/2$  by  $N_2/2$  by  $N_3/2$ . This is illustrated in Fig 1. The

separable 3D DWT of a signal is implemented by iterating the 3D analysis filter bank on the lowpass subband data. (<http://taco.poly.edu/WaveletSoftware/>)

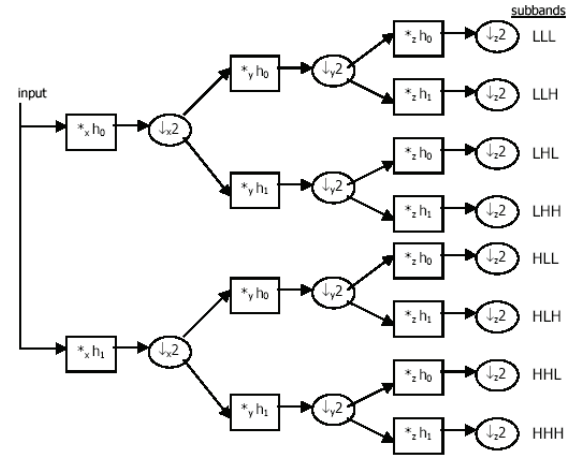


**Fig 1.** Block diagram of a single level decomposition for the 3D DWT. (<http://taco.poly.edu/WaveletSoftware/>)

The aim of MMA method proposed by Boussion *et al* [3] is to decompose both MRI and PET images into a successive details layers  $W_i$  (wavelet coefficients) using a wavelet tranform in order to introduce the high frequency information of the anatomical image into the functional image. Nevertheless, the anatomical details (high frequency MRI wavelet coefficients) can not be directly replaced into the functional image since they do not have the same spatial resolution neither the same wavelet coefficient intensities.

In this work a new algorithm based on wavelet analysis was implemented. Firstly, both anatomic and functional images are decomposed into successive details layers  $w_i$  (wavelet coefficients) by using the 3D-DWT (symmlets 4; second decomposition level). As a second step, an energy model is established between the anatomic and functional details at a common frequency domain level. In this model, a global energy parameter was calculated in order to achieve the final required information in the corrected image:

a) firstly, low frequencies of PET should be preserved since they correspond to the functional contrasts;

b) Moreover, the corrected PET image must present the higher spatial resolution of the MRI;

To achieve a corrected image with these two requirements, a simple energy global factor is proposed. The energy of high and low frequency details of each image were calculated:

$$E_{PET|MRI_H} = \sum w_{PET|MRI_H}^2 \quad \text{and} \quad E_{PET|MRI_L} = \sum w_{PET|MRI_L}^2 \quad (1)$$

where  $w$  are the wavelet coefficients at a second decomposition level. Then the ratio between the high and low information of the MRI was calculated in (2) in order to understand the weight of its high frequency information in the global image and consequently its high spatial resolution level.

$$r_{MRI} = \frac{E_{MRI_L}}{E_{MRI_H}} \quad (2)$$

The global energy factor was determined and applied to the high frequency details of the MRI in order to be able to replace them into the PET image. The global energy factor consists in keeping the PET low frequency information in the corrected image and, in the other hand, replace the PET high frequency details by those of the MRI keeping the ratio between the high and low information of the MRI in the new corrected image.

$$r_{final} = \frac{E_{final_L}}{E_{final_H}} \rightarrow \frac{E_{PET_L}}{E_{new det ails_H}} \rightarrow \frac{E_{PET_L}}{R_{energy} \times E_{MRI_H}}, \text{ where}$$

$$R_{energy} = \frac{E_{PET_L}}{r_{MRI} \times E_{MRI_H}} \quad (3)$$

Finally, the new high frequency details are introduced into the initial functional image in order to obtain those that are lacking, as shown bellow.

$$w_{PET_{cor}} = w_{PET_L} + \sqrt{R_{energy}} \times w_{MRI_H} \quad (4)$$

### B. Performance

To validate the performance of the new PVC design, regarding the quantitative measurements, the NEMA Image Quality phantom was used (NEMA NU 4-2008 for small animal PET systems) [5]. The phantom is made of polymethylmethacrylate and its main body is composed of a cylindrical chamber with 30 mm diameter and 30 mm length. The remaining 20 mm of the phantom body length is solid with 5 fillable rods with diameters of 1, 2, 3, 4 and 5 mm, respectively. A lid that attaches to the large uniform region end of the phantom supports two cold region chambers. One of these chambers was filled with non-radioactive water. The radionuclide employed for these measurements was  $^{18}\text{F}$ . The activity used, as reference, in the whole phantom was 100  $\mu\text{Ci}$ , since it is within the range of the total activity used in most of the mouse studies. To generate the anatomical image a binary matrix was created to define the contrast between hot and cold regions (binary image).

In order to demonstrate the use of the algorithm in clinical context, the technique was also applied to a  $^{18}\text{F}$ -FDG study of a patient with severe leukariosis, having already a T-1 weighted 3D MRI scan. PET images were acquired using an ECAT EXACT HR+ scanner. The  $^{18}\text{F}$ -FDG image was acquired in 3D mode and reconstructed using 2D FBP (Hann filter cutoff-frequency 4.9 mm FWHM) with Fourier rebinning (FORE). The T-1 weighted 3D MRI scan was spatially co-registered with the functional PET data. An axial three-dimensional spoiled gradient-echo sequence with the following parameters: repetition time, 25 ms; echo time, 6 ms; flip angle, 28°; field of view, 25 × 25 cm; matrix size, 256 × 256; section thickness, 2 mm with no interslice gap; and number of excitations, 1.

## III. RESULTS

Fig 2 presents the initial phantom image and the corrected phantom image after PVE correction using the proposed algorithm. As it can be observed, the corrected image presents a higher spatial resolution and all the resultant sphere limits are well defined.

Table I shows the quantitative results obtained of the proposed PVC algorithm and it presents the theoretical, observed and after PVC ROI means of the 5 rods in the phantom, the uniform cylinder chamber, the water cylinder chamber and the background. The quantitative results show that the combination of MMA and the energy image analysis leads to a significant recovery of lost intensity induced by PVE. Even the cylinders of very small diameter present a high recovery of their values. The correction of spill-over was also analyzed, and as it can be observed in Table I, the over estimation observed on cold regions (water cylinder chamber) was also recovered. Nevertheless, the proposed algorithm introduces an artifact in the resultant corrected images (Fig 2(c)).

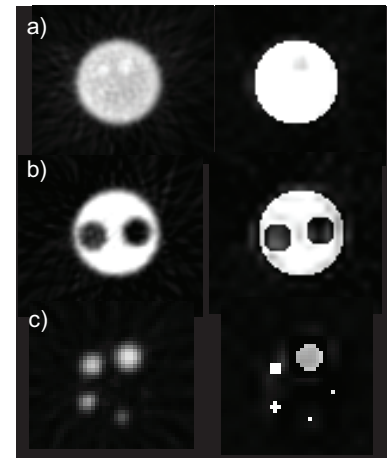


**Fig 2.** The initial image and the corrected one after PVE correction using the proposed algorithm: (a) the 5 rods drilled of the phantom; (b) the uniform cylinder chamber; (c) the water cylinder chamber.



**Table I.** Theoretical, observed and after PVE correction using the proposed algorithm ROI means of the 5 rods drilled in the phantom, the uniform cylinder chamber, the water cylinder chamber and the background. Recovery and Spill-over Coefficient values.

Recovery Coefficients (mean $\pm$ SD)					
ROI (diameter)	Theoretical Mean	Observed Mean	RC before PVC	Corrected Mean	RC after PVC
1 mm	100	11,294 $\pm$ 11,58	0,11	97,552 $\pm$ 10,84	0,98
2 mm	100	32,076 $\pm$ 7,48	0,32	105,808 $\pm$ 8,67	1,06
3 mm	100	38,871 $\pm$ 9,76	0,39	87,516 $\pm$ 12,87	0,88
4 mm	100	56,447 $\pm$ 5,74	0,56	106,204 $\pm$ 11,12	1,06
5 mm	100	58,535 $\pm$ 9,36	0,59	92,837 $\pm$ 12,54	0,93
30 mm	100	80,879 $\pm$ 7,35	0,81	89,615 $\pm$ 17,25	0,90
Spill-over (mean $\pm$ SD)					
Water ( 8 mm)	0	17,018 $\pm$ 15,95	17,02	-4,835 $\pm$ 23,80	-4,84
Background	0	0,00 $\pm$ 6,59	0,00	-0,192 $\pm$ 5,18	-0,19

Fig 3 shows an application of the proposed PVC method on a human pathological  $^{18}\text{F}$ -FDG PET brain data. Visually, the corrected image showed enhanced resolution, includes all the FDG uptake information and presents a significant higher spatial resolution. The proposed PVC method involving an analysis of both anatomic and functional image energies shows that with one single parameter, the global energy factor, it is possible to achieve a common frequency level between MRI and PET images and therefore be enable to use and replace the high frequency information in the PET image. The proposed PVC method is applicable without making any prior assumptions on the content of the functional images, and therefore it can be applied to normal and pathological datasets.

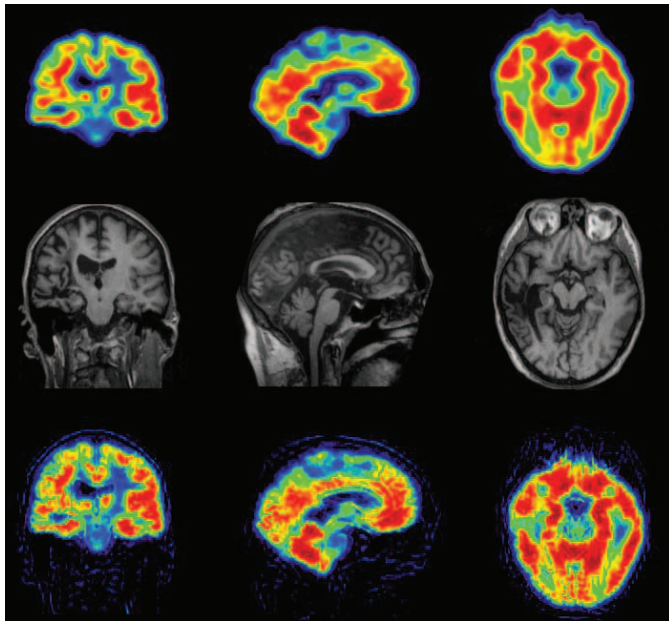


**Fig 3.** (up to down) Clinical  $^{18}\text{F}$ -FDG PET image; T-1 image; and the corrected clinical PET image after PVE correction using the proposed algorithm.

#### IV. CONCLUSIONS

This study demonstrates that the proposed PVC method is a strong tool for correcting PVE in funtional images. Results from this work are encouraging. Using the anatomical image information (MRI or CT) it is possible to introduce high

frequency details in the funtional image improving its spatial resolution and subsequently leading to a significant recovery of lost intensity induced by PVE. Moreover, the PVC algorithm presented here do not require an *a priori* information regarding to the PET image distribution.

The MMA method has its own limitations, using a MMA algorithm a optimal co-registration between PET and MRI or CT is mandatory and sometimes it is difficult to achieve because of patient physiological motion as well as patient uncontrollable movement during image acquisitions.

Future work will consist in further pursuing technical and clinical validation through the use of extended clinical and simulated databases. In addition, intensity recovery and resultant artifact of the corrected image could probably be improved by the use of more accurate and powerful wavelet transforms, e.g., the dual-tree complex wavelet transform (CWT).

#### REFERENCES

- [1] O. G. Rousset, Y. Ma, and A. C. Evans, "Correction for partial volume effects in PET: principle and validation," *J Nucl Med*, vol. 39, pp. 904-11, May 1998.
- [2] N. Boussion, C. Cheze Le Rest, M. Hatt, and D. Visvikis, "Incorporation of wavelet-based denoising in iterative deconvolution for partial volume correction in whole-body PET imaging," *Eur J Nucl Med Mol Imaging*, vol. 36, pp. 1064-75, Jul 2009.
- [3] N. Boussion, M. Hatt, F. Lamare, Y. Bizais, A. Turzo, C. Cheze-Le Rest, and D. Visvikis, "A multiresolution image based approach for correction of partial volume effects in emission tomography," *Phys Med Biol*, vol. 51, pp. 1857-76, Apr 7 2006.
- [4] M. Shidahara, C. Tsoumpas, A. Hammers, N. Boussion, D. Visvikis, T. Suhara, I. Kanno, and F. E. Turkheimer, "Functional and structural synergy for resolution recovery and partial volume correction in brain PET," *Neuroimage*, vol. 44, pp. 340-8, Jan 15 2009.
- [5] National Electrical Manufacturers Association. Performance measurements of Small Animal Positron Emission Tomographs. Rosslyn VA; 2008 Standards Publication NU 4-2008. <http://www.nema.org/stds/nu4.cfm>